


# Scrambling Dynamics across a Thermalization-Localization Quantum Phase Transition

Subhayan Sahu,<sup>1</sup> Shenglong Xu<sup>1</sup>,<sup>✉</sup> and Brian Swingle<sup>2</sup>

<sup>1</sup>*Condensed Matter Theory Center and Department of Physics, University of Maryland, College Park, Maryland 20742, USA*

<sup>2</sup>*Condensed Matter Theory Center, Maryland Center for Fundamental Physics, Joint Center for Quantum Information and Computer Science, and Department of Physics, University of Maryland, College Park, Maryland 20742, USA*

 (Received 7 December 2018; revised manuscript received 17 August 2019; published 18 October 2019)

We study quantum information scrambling, specifically the growth of Heisenberg operators, in large disordered spin chains using matrix product operator dynamics to scan across the thermalization-localization quantum phase transition. We observe ballistic operator growth for weak disorder, and a sharp transition to a phase with subballistic operator spreading. The critical disorder strength for the ballistic to subballistic transition is well below the many body localization phase transition, as determined from finite size scaling of energy eigenstate entanglement entropy in small chains. In contrast, we find that the transition from subballistic to logarithmic behavior at the actual eigenstate localization transition is not resolved in our finite numerics. These data are discussed in the context of a universal form for the growing operator shape and substantiated with a simple phenomenological model of rare regions.

DOI: [10.1103/PhysRevLett.123.165902](https://doi.org/10.1103/PhysRevLett.123.165902)

It has long been known that disorder can slow or arrest quantum motion [1], leading to a localized state. Recently it was understood that localization can survive even strong interactions, a phenomenon dubbed many-body localization (MBL) [2–4]. More precisely, there is a quantum phase transition in interacting systems from a thermalizing phase to a localized phase with increasing disorder. The phase and phase transition have been intensely studied (e.g., [5–20]), and there is a proof, given plausible assumptions, of the existence of MBL in one-dimensional spin chains with local interactions [21,22].

In this Letter we are particularly concerned with the quantum phase transition (or transitions) that take a one-dimensional disordered system from a thermalizing phase to a localized phase [9,12,23–29]. It is natural to study this phase transition via dynamics [6–8,10], because eigenstate based numerics are difficult to scale to large system sizes and because dynamical properties are accessible in experiments [30–32]. We study a dynamical quantity related to quantum information scrambling, the squared commutator [33–36].

Consider two local operators,  $W$  and  $V$ , in a one-dimensional spin chain, separated by a distance  $x$ . The squared commutator probes the extent to which  $V$  fails to commute with the time evolved Heisenberg operator  $W(t) = e^{iHt} W e^{-iHt}$ . It is defined as the expectation value of the absolute value squared of the commutator of the  $W(t)$  and  $V$ ,

$$C(x, t) = \langle [W(t), V]^\dagger [W(t), V] \rangle. \quad (1)$$

It is closely related to the out of time ordered correlator (OTOC),  $F(t) = \langle W^\dagger(t) V W^\dagger(t) V \rangle$ . OTOCs are currently

receiving attention as a diagnostic of quantum chaos [33,37–39], including experimental proposals [40–43] and early experiments measuring OTOCs [44–47]. In fact, [46] measured OTOCs detect localization in NMR spin systems.

The squared commutator starts at zero for initially separated  $W$  and  $V$ , and then grows as the operator  $W(t)$  spreads and overlaps with the location of  $V$ . In the absence of disorder,  $C(x, t)$  typically grows ballistically, leading to an emergent linear light cone with butterfly velocity  $v_B$ . On the other hand, disorder can severely arrest the growth of  $C(x, t)$ , a manifestation of localization. It has been argued that MBL is characterized by an extensive number of local integrals of motion [11–14], leading to an emergent logarithmic light cone [48]. Similarly, it was recently shown that the disorder averaged  $C(x, t)$  exhibits a logarithmic light cone with  $v_B = 0$  in the MBL phase [49–55].

In this Letter we study operator dynamics across the entire thermal-to-MBL phase diagram, with a particular focus on the thermal side of the MBL eigenstate transition. This regime has attracted interest in the context of rare region effects which can slow down transport well before the MBL transition [15,16,56,57]. One interesting question is whether the butterfly velocity survives arbitrarily weak disorder [58,59]. It is challenging, since, for example, strong disorder RG [55] applies only in the MBL phase and state-of-the-art exact diagonalization is still limited to small sizes [58]. We use a recent time-dependent density matrix renormalization group (DMRG) based matrix product operator method to calculate dynamics of local Heisenberg operators [60] (see also [61,62]) for larger system sizes [ $\mathcal{O}(200)$  spins] and longer times than previously possible.

First, we observe a weak disorder phase with ballistic operator spreading ( $v_B \neq 0$ ) as well as a sharp transition to a sub-ballistic phase ( $v_B = 0$ ), at a disorder strength well below the putative MBL transition. This transition is characterized by a continuous vanishing of  $v_B$  and an apparent divergence of the wave front broadening. Second, we study the variability of operator growth from one disorder realization to another, which also characterize the ballistic to subballistic transition independent of the fitting procedure. This is also a clear numerical demonstration of rare regions that are only possible because of the large system size. Observations from the variability of the scrambling data motivate a simple phenomenological model of rare regions, from which we analytically substantiate the presence of the ballistic phase. Together these numerical observations reveal a rich dynamical phase diagram for disordered spin models (Fig. 1). Comparing to previous studies, we find that the loss of ballistic operator spreading occurs at a larger disorder strength than the diffusive to sub-diffusive transition in spin transport, indicating at least four nontrivial dynamical regimes [15,16,56,57,59,63].

*Model.*—For concreteness, we consider two one-dimensional spin chain models: (1) mixed field Ising model with  $\sigma^z$  disorder,

$$H = -J \sum_{r=1}^{L-1} Z_r Z_{r+1} - h_x \sum_{r=1}^L X_r - \sum_{r=1}^L h_{z,r} Z_r, \quad (2)$$

(2) Heisenberg model with  $\sigma^z$  disorder,

$$H = -J \sum_{r=1}^{L-1} (X_r X_{r+1} + Y_r Y_{r+1} + Z_r Z_{r+1}) - \sum_{r=1}^L h_{z,r} Z_r. \quad (3)$$

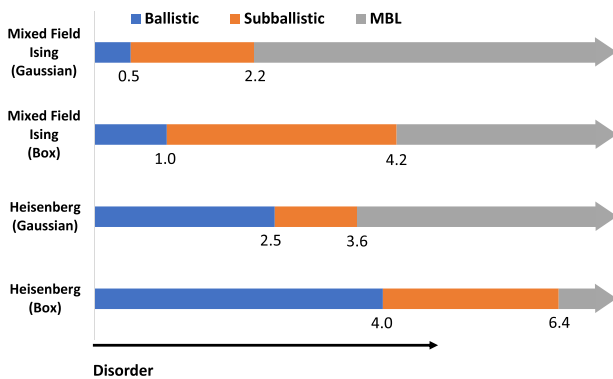


FIG. 1. Phase diagram of operator spreading in disordered interacting spin systems with different disorder models. The Heisenberg Hamiltonian is defined using Pauli operators instead of spin-1/2 operators, so the  $W$  normalization is twice as large relative to the spin-1/2 convention.

Here  $X_r, Y_r, Z_r$  are the local Pauli operators. For the mixed field Ising model, we choose the parameters  $J = 1$ ,  $h_x = 1.05$ , and  $\overline{h_{z,r}} = 0.5$ . For the Heisenberg model, we choose the parameters  $J = 1$  and  $\overline{h_{z,r}} = 0$ . For each spin chain we consider two different disorder probability distributions, box and Gaussian. For the box disorder, we draw the  $h_{z,r}$  fields uniformly at random from the interval  $[-W, W]$ , with  $W$  being the disorder strength. For Gaussian disorder, the  $h_{z,r}$  fields are Gaussian random variables with standard deviation (SD)  $W$ . The parameters for the mixed field Ising model have been chosen so that the  $W = 0$  limit is strongly chaotic [60]. The Heisenberg model with box disorder has been extensively studied for chains with  $L \lesssim 30$  spins, and it has been shown that the thermal-MBL transition occurs at  $W \gtrsim 7$  [17]. We consider all these models to elucidate the robustness of the intermediate regime, and also to understand the role of disorder distribution on rare region effects.

*Method.*—Our technique is a real-time tensor network method for operator dynamics [60]. Studying real-time quantum dynamics using tensor network methods, such as state-based time evolving block decimation (TEBD) or t-DMRG methods [7,8,64–67], is typically limited to early times, because the entanglement of the state is upper bounded by  $\log(\chi)$ , where  $\chi$  is the bond dimension of the matrix product state (MPS) [7]. However, in a recent paper [60], some of us have shown that by going to the Heisenberg picture, one can reliably access a much wider space-time region using dynamics of matrix product operators (MPO) because of the entanglement structure of the Heisenberg operator. The complexity of the operator only builds up within the light cone and is not essential for studying the dynamical property of the wave front. As a result, the butterfly velocity and the broadening of the wave front can be accurately extracted from TEBD simulation on Heisenberg operators in the matrix product form with modest bond dimension.

We simulated the squared commutator in the infinite temperature Gibbs ensemble,

$$C(r - r', t) = \frac{1}{2L} \text{tr}([X_r(t), X_{r'}]^\dagger [X_r(t), X_{r'}]) \quad (4)$$

for spin chains of length  $L = 201$  with maximal time of order 50–100, in the units of  $J^{-1} = 1$ . A small Trotter step of  $\delta t = 0.0025$  is used to obtain high numerical precision. For each disorder, we consider around 200–500 disorder realizations and average  $\log(C)$  over the different realizations. This ensures that rare disorder realizations that could localize the operator growth are not overwhelmed by the ballistic samples during the averaging process. Figure 2 shows light cone obtained from averaging  $C(x, t)$  for different disorders, representing each phase in Fig. 1. We discuss convergence of the numerical procedure in Sec. I of the Supplemental Material [68].

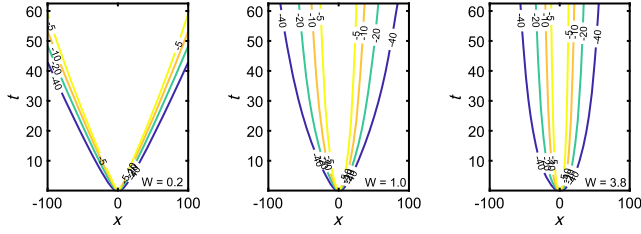


FIG. 2. Plot of the contours of the averaged  $\log(C)$ , for the mixed field Ising model with Gaussian disorder. Averaged over  $\sim 200$  disorder realizations, for three disorders,  $W = 0.2$  (ballistic),  $W = 1.0$  (intermediate), and  $W = 3.8$  (logarithmic). Bond dimension is 32. Convergence with bond dimension is discussed in the Supplemental Material [68]. Fluctuations away from the disorder averaging are discussed in Fig. 4 and in the corresponding section.)

We detect the transition by extracting the butterfly velocity and the wave front broadening from the averaged squared commutator. We use the universal form for the squared commutator ahead of the wave front [where  $C(x, t) \ll 1$ ], conjectured in [60,62,69],

$$C(x, t) \sim \exp(-\lambda_p(x - v_B t)^{1+p}/t^p) \quad (5)$$

Here,  $v_B$  is the butterfly velocity, and  $p$  is the wave front broadening coefficient, which is known to be  $p = 1$  for random unitary circuit models [70,71],  $p = 0$  for large- $N$  holographic models and  $p = \frac{1}{2}$  for noninteracting systems. The above form does not hold in the localized regime, which has a logarithmic light cone [49–55]. Additionally, the shape of the light cone becomes power-law-like before the MBL transition due to rare region effects [58,59]. A general form that captures all the scenarios is,

$$C(x, t) \sim \exp(-\lambda_p(x - v_B t)^{1+p}/t^p + a \log(t)) \quad (6)$$

This form captures the cases where the light cone is linear ( $v_B \neq 0$ ,  $a = 0$ ), power law ( $v_B = 0$ ,  $p \neq 0$ ,  $a = 0$ ), or logarithmic ( $p = 0$ ,  $v_B = 0$ ,  $a \neq 0$ ), as the disorder strength increases.

*Numerical result.*—Here we use the mixed-field Ising model with Gaussian disorder as an example to demonstrate the transitions in Fig. 1. The other three cases can be found in the Supplemental Material [68]. In Fig. 3, we plot the extracted  $v_B$  and  $p$  versus disorder, for different lengths of the spin chain by fitting the data to the growth form (5). The fitting procedure and the goodness of fit are discussed in the Supplemental Material, Sec. II. The butterfly velocity decreases as the disorder strength increases and becomes zero at  $W \sim 0.5$ . On the other hand,  $p$  increases as  $W$  approaches the critical disorder, and decreases when  $W$  passes beyond that. This disorder is below the MBL transition disorder extracted from the exact diagonalization

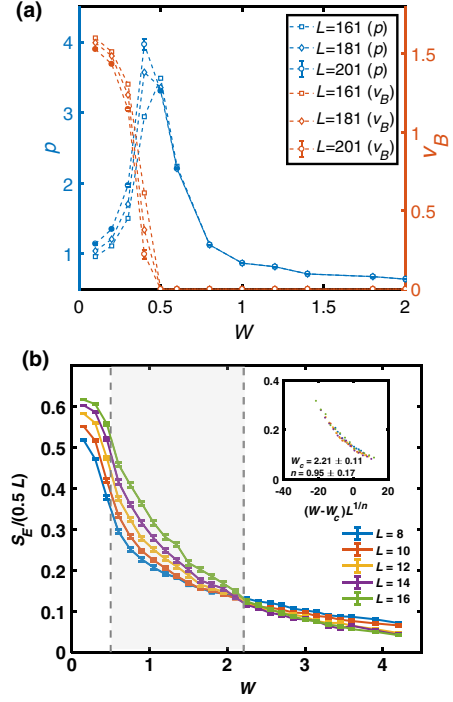


FIG. 3. (a) The extracted broadening coefficient  $p$  and butterfly velocity  $v_B$  are plotted for different sized systems, versus disorder. Note,  $v_B$  goes to zero and  $p$  has a peak at around disorder  $W \sim 0.5$  with small finite-size effect. Error bars obtained from the 95% confidence interval of fitting, are shown for the largest system size. (b) Finite-size scaling on half-chain entanglement entropy estimates that the localization transition occurs at  $W_c \sim 2.21$ . The data collapse to the degree 3 polynomial ansatz  $g[(W - W_c)L^{1/n}]$  with  $n \sim 0.95$  is shown in the inset. The shaded region is the intermediate region.

study on the entanglement entropy scaling [Fig. 3(b)]. The fact that  $v_B$  goes to zero and  $p$  peaks at the same disorder strength indicates a sharp transition before the true MBL transition, consistent with the weak-link model describing the rare region effects in disordered systems, studied recently [59].

Below the transition, the system is characterized by a finite  $v_B$  and  $p$ , indicating a linear light cone with broadening front. Above the transition, the velocity becomes zero and the shape of the light cone becomes power-law-like,  $x \sim t^{p/(p+1)}$ . Our method captures the logarithmic light cone in the strong disorder limit [Fig. 2(c)], but it is difficult to ascertain the transition to the logarithmic light cone from fitting the finite space-time data. This is discussed in the Supplemental Material [68], Sec. II, where we also provide more evidence of logarithmic light cones at a high disorder strength beyond the MBL transition. The transition identified here is different from the diffusive-subdiffusive transition for dynamics of conserved quantities [56,63]. In particular, we observe that in the Heisenberg model with box disorder, the  $v_B = 0$  transition occurs at a higher disorder,  $W \sim 4$  than the spin transport

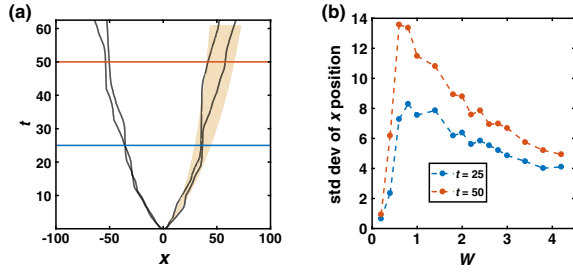


FIG. 4. (a) The bold black lines are *single realizations* of  $-15$  contour lines of  $\log(C)$  at disorder  $W = 0.8$  for the mixed field Ising model with Gaussian disorder. Note the colored patch is given by the SD of the  $x$  positions for 180 realizations at a given time. Note that the two disorder realizations have distinct behaviors after  $t = 25$ , with one being significantly slower because of a local bottleneck of large disorder. (b) SD of  $x$  cuts at times  $t = 25$  and  $t = 50$ , for 180 realizations for different disorders are plotted, which peaks at  $W \sim 0.5$  and coincides with the critical disorder where  $v_B$  vanishes.

diffusive-subdiffusive transition disorder,  $W \sim 1.1$  (from [56], in our Pauli matrix convention). This implies a separation of information propagation and spin transport.

*Shot to shot variability.*— We also study the variability of the contours of  $\log(C)$  from one disorder realization to another. In Fig. 4(a) a particular contour line of  $\log(C)$  is plotted for two different disorder realizations with  $W = 0.8$  which differ significantly. To characterize the shot to shot fluctuations, in Fig. 4(b), we plot the SD of  $x$  positions, and observe that, at long time, the variability peaks at the same disorder ( $W \sim 0.5$ ) where  $v_B$  vanishes. The divergence of fluctuations, obtained without any numerical fitting, is remarkably consistent with the divergence of  $p$  in Fig. 3(a). This substantiates the transition at  $W \sim 0.5$ . Figure 4(a) also demonstrates the microscopic mechanism for vanishing  $v_B$  before the MBL eigenstate transition. The contours for two different realizations have bottlenecks at certain space regions, where scrambling is arrested. This is a visualization of rare region effects—local stronger disorders in certain regions affecting average dynamical properties.

*Rare region model.*—Motivated by above numerical results, we construct a simple model of rare regions which explains the emergence of power law, broadening behavior, and the existence of a ballistic phase at weak disorders. In a  $L$  sized spin chain with Gaussian random disorders  $\mathcal{N}(0, \sigma^2)$ , the SD of local disorder, might be different from  $\sigma$ . It might also exceed the MBL critical disorder  $\epsilon_c$ , even when  $\sigma < \epsilon_c$ . Let  $\epsilon$  be the disorder beyond which the operator growth has a logarithmic light cone. Consider a continuous stretch of  $\alpha \log(L)$  spins, whose SD exceeds  $\epsilon$ . The balance between the exponentially slow transport and logarithmic size of such region leads to overall subballistic information transport. Specifically, the time it takes for the information to propagate across the chain with one such

rare region is  $t \sim L/v_B + e^{\zeta \alpha \log L}$ , where  $\zeta$  is treated as the averaged inverse length scale associated with the logarithmic cone for the current purpose (it is defined carefully in the Supplemental Material [68] Sec. V). In the limit  $L \rightarrow \infty$ , the average velocity  $L/t$  goes to zero for  $\zeta \alpha > 1$ , indicating the subballistic scenario. This corresponds to the case where the rare region is long enough that it dominates the time,  $t \sim L^{\zeta \alpha}$ . As the ballistic transition is approached, we have  $\zeta \alpha \rightarrow 1^+$ . Comparing to the power-law light cone  $x \sim t^{p/(p+1)}$  indicates that  $p \rightarrow \infty$ , which is consistent with the apparent divergence of  $p$  at the ballistic-subballistic transition in our numerical result. A related but distinct approach was considered in [59], where the rare region effects on operator spreading were quantified using a coarse grained quantity related to the entanglement spreading across weak links. Our model is directly in terms of the bare disorder and gives rise to consistent predictions.

The existence of a ballistic phase in the low disorder limit is also borne out of the simple model. Consider the probability of having *no* rare region of length  $\alpha \log L$  with SD larger than  $\epsilon$  in a disordered spin chain of length  $L$  with global SD  $\sigma$ , denoted as  $q(\alpha; \sigma, \epsilon)$ . In general,  $q$  decreases with  $\sigma$  and increases with  $\alpha$ . Based on the above discussion, any  $\alpha$  larger than  $1/\zeta$  leads to subballistic slowing down of the information propagation. Therefore, a sufficient condition for ballistic propagation is that no such disruptive rare regions occur, i.e.,  $q(1/\zeta; \sigma, \epsilon) = 1$ . In Sec. V of the Supplemental Material [68], we prove the following inequality,

$$q(1/\zeta; \sigma, \epsilon) \geq (1 - \beta^{\log(L)/\zeta})^{\{\zeta L\}/\log(L)} \quad (7)$$

where  $\beta = [(e^2/\sigma^2)e^{1-(e^2/\sigma^2)}]^{1/2}$ . In the limit,  $L \rightarrow \infty$ , the RHS of Eq. (7) is 1 when  $\beta < e^{-\zeta}$ . In terms of microscopic parameters, the condition becomes,

$$\frac{\epsilon^2}{\sigma^2} e^{1-(e^2/\sigma^2)} < e^{-2\zeta}. \quad (8)$$

Since  $\zeta$  is finite, there exists a finite  $\sigma^*$ , below which all  $\sigma$  satisfy the sufficient condition for ballistic transport Eq. (8), leading to a finite window of a ballistic phase.

It is worth noting that the model only shows the existence of a ballistic phase for  $\sigma < \sigma^*$ . The inequality is a sufficient, but not a necessary condition for ballistic transport; hence  $\sigma^*$  should not be mistaken with the critical ballistic-subballistic transition. Furthermore, in our numerics, we can't resolve  $\epsilon$ , where subballistic becomes logarithmic (in a finite system data, a soft power law is difficult to resolve from a logarithm), or  $\zeta$  which will be a complicated averaged scale. Hence we can't quantitatively verify Eq. (8). A more careful study of the difference between the average time  $\bar{t}$  and the typical time  $\exp(\overline{\log t})$  should be considered to further characterize the ballistic to subballistic transition.



*Conclusions.*—We studied the ballistic to subballistic crossover in operator spreading for large interacting disordered spin systems using MPO dynamics for different spin Hamiltonians and error models. Our numerical results establish the existence of a ballistic phase and a sharp transition to a subballistic phase. The numerical observation of fluctuations of the wave front motivate a simple model of rare regions which explains aspects of this transition. Natural extensions of the rare region model would be to incorporate the effects of wave front broadening into the analysis. Also our work demonstrates a separation between information propagation and spin transport [56,63], which could be an interesting direction of future study.

We acknowledge the University of Maryland supercomputing resources, specifically the DeepThought2 cluster, used in this work. We also thank D. Huse, V. Khemani, and S. Gopalakrishnan for discussions. This material is based on work supported by the Simons Foundation via the It From Qubit Collaboration, by the Air Force Office of Scientific Research (FA9550-17-1-0180), and by the NSF Physics Frontier Center at the Joint Quantum Institute (PHY-1430094).

- 
- [1] P. W. Anderson, *Phys. Rev.* **109**, 1492 (1958).  
 [2] D. M. Basko, I. L. Aleiner, and B. L. Altshuler, *Ann. Phys. (Amsterdam)* **321**, 1126 (2006).  
 [3] V. Oganesyan and D. A. Huse, *Phys. Rev. B* **75**, 155111 (2007).  
 [4] I. V. Gornyi, A. D. Mirlin, and D. G. Polyakov, *Phys. Rev. Lett.* **95**, 206603 (2005).  
 [5] A. Pal and D. A. Huse, *Phys. Rev. B* **82**, 174411 (2010).  
 [6] M. Žnidarič, T. Prosen, and P. Prelovšek, *Phys. Rev. B* **77**, 064426 (2008).  
 [7] J. H. Bardarson, F. Pollmann, and J. E. Moore, *Phys. Rev. Lett.* **109**, 017202 (2012).  
 [8] M. Serbyn, Z. Papić, and D. A. Abanin, *Phys. Rev. Lett.* **110**, 260601 (2013).  
 [9] B. Bauer and C. Nayak, *J. Stat. Mech.* (2013) P09005.  
 [10] E. Altman and R. Vosk, *Annu. Rev. Condens. Matter Phys.* **6**, 383 (2015).  
 [11] M. Serbyn, Z. Papić, and D. A. Abanin, *Phys. Rev. Lett.* **111**, 127201 (2013).  
 [12] R. Vosk, D. A. Huse, and E. Altman, *Phys. Rev. X* **5**, 031032 (2015).  
 [13] D. A. Huse, R. Nandkishore, and V. Oganesyan, *Phys. Rev. B* **90**, 174202 (2014).  
 [14] B. Swingle, [arXiv:1307.0507](https://arxiv.org/abs/1307.0507).  
 [15] K. Agarwal, S. Gopalakrishnan, M. Knap, M. Müller, and E. Demler, *Phys. Rev. Lett.* **114**, 160401 (2015).  
 [16] K. Agarwal, E. Altman, E. Demler, S. Gopalakrishnan, D. A. Huse, and M. Knap, *Ann. Phys. (Berlin)* **529**, 1600326 (2017).  
 [17] D. J. Luitz, N. Laflorencie, and F. Alet, *Phys. Rev. B* **91**, 081103 (2015).  
 [18] R. Nandkishore and D. A. Huse, *Annu. Rev. Condens. Matter Phys.* **6**, 15 (2015).  
 [19] A. C. Potter, R. Vasseur, and S. A. Parameswaran, *Phys. Rev. X* **5**, 031033 (2015).  
 [20] D. A. Abanin and P. Zlatko, *Ann. Phys. (Berlin)* **529**, 1700169 (2017).  
 [21] J. Z. Imbrie, *Phys. Rev. Lett.* **117**, 027201 (2016).  
 [22] J. Z. Imbrie, *J. Stat. Phys.* **163**, 998 (2016).  
 [23] D. A. Huse, R. Nandkishore, V. Oganesyan, A. Pal, and S. L. Sondhi, *Phys. Rev. B* **88**, 014206 (2013).  
 [24] A. Chandran, V. Khemani, C. R. Laumann, and S. L. Sondhi, *Phys. Rev. B* **89**, 144201 (2014).  
 [25] D. Pekker, G. Refael, E. Altman, E. Demler, and V. Oganesyan, *Phys. Rev. X* **4**, 011052 (2014).  
 [26] J. A. Kjäll, J. H. Bardarson, and F. Pollmann, *Phys. Rev. Lett.* **113**, 107204 (2014).  
 [27] T. Grover, [arXiv:1405.1471](https://arxiv.org/abs/1405.1471).  
 [28] Y. Bahri, R. Vosk, E. Altman, and A. Vishwanath, *Nat. Commun.* **6**, 7341 (2015).  
 [29] V. Khemani, S. P. Lim, D. N. Sheng, and D. A. Huse, *Phys. Rev. X* **7**, 021013 (2017).  
 [30] A. Rubio-Abadal, J.-y. Choi, J. Zeiher, S. Hollerith, J. Rui, I. Bloch, and C. Gross, [arXiv:1805.00056](https://arxiv.org/abs/1805.00056).  
 [31] H. P. Lüschen, P. Bordia, S. Scherg, F. Alet, E. Altman, U. Schneider, and I. Bloch, *Phys. Rev. Lett.* **119**, 260401 (2017).  
 [32] H. P. Lüschen, P. Bordia, S. S. Hodgman, M. Schreiber, S. Sarkar, A. J. Daley, M. H. Fischer, E. Altman, I. Bloch, and U. Schneider, *Phys. Rev. X* **7**, 011034 (2017).  
 [33] S. H. Shenker and D. Stanford, *J. High Energy Phys.* **3** (2014) 67.  
 [34] P. Hayden and J. Preskill, *J. High Energy Phys.* **09** (2007) 120.  
 [35] Y. Sekino and L. Susskind, *J. High Energy Phys.* **10** (2008) 065.  
 [36] P. Hosur, X.-L. Qi, D. A. Roberts, and B. Yoshida, *J. High Energy Phys.* **2** (2016) 004.  
 [37] A. I. Larkin and Y. N. Ovchinnikov, *Sov. Phys. JETP* **28**, 1200 (1969).  
 [38] A. Kitaev, A simple model of quantum holography, KITP Strings Seminar and Entanglement 2015 Program, 2015.  
 [39] J. Maldacena, S. H. Shenker, and D. Stanford, *J. High Energy Phys.* **8** (2016) 106.  
 [40] B. Swingle, G. Bentsen, M. Schleier-Smith, and P. Hayden, *Phys. Rev. A* **94**, 040302 (2016).  
 [41] G. Zhu, M. Hafezi, and T. Grover, *Phys. Rev. A* **94**, 062329 (2016).  
 [42] N. Y. Yao, F. Grusdt, B. Swingle, M. D. Lukin, D. M. Stamper-Kurn, J. E. Moore, and E. A. Demler, [arXiv:1607.01801](https://arxiv.org/abs/1607.01801).  
 [43] N. Yunger Halpern, *Phys. Rev. A* **95**, 012120 (2017).  
 [44] J. Li, R. Fan, H. Wang, B. Ye, B. Zeng, H. Zhai, X. Peng, and J. Du, *Phys. Rev. X* **7**, 031011 (2017).  
 [45] M. Garttner, J. G. Bohnet, A. Safavi-Naini, M. L. Wall, J. J. Bollinger, and A. M. Rey, *Nat. Phys.* **13**, 781 (2017).  
 [46] K. X. Wei, C. Ramanathan, and P. Cappellaro, *Phys. Rev. Lett.* **120**, 070501 (2018).  
 [47] E. J. Meier, J. Ang'ong'a, F. A. An, and B. Gadway, *Phys. Rev. A* **100**, 013623 (2019).

- [48] C. K. Burrell and T. J. Osborne, *Phys. Rev. Lett.* **99**, 167201 (2007).
- [49] B. Swingle and D. Chowdhury, *Phys. Rev. B* **95**, 060201 (2017).
- [50] Y. Huang, Y. L. Zhang, and X. Chen, *Ann. Phys. (Berlin)* **529**, 1600318 (2017).
- [51] R. Fan, P. Zhang, H. Shen, and H. Zhai, *Sci. Bull.* **62**, 707 (2017).
- [52] R. Q. He and Z. Y. Lu, *Phys. Rev. B* **95**, 054201 (2017).
- [53] Y. Chen, [arXiv:1608.02765](https://arxiv.org/abs/1608.02765).
- [54] X. Chen, T. Zhou, D. A. Huse, and E. Fradkin, *Ann. Phys. (Berlin)* **529**, 1600332 (2017).
- [55] K. Slagle, Z. Bi, Y. Z. You, and C. Xu, *Phys. Rev. B* **95**, 165136 (2017).
- [56] M. Žnidarič, A. Scardicchio, and V. K. Varma, *Phys. Rev. Lett.* **117**, 040601 (2016).
- [57] I. Khait, S. Gazit, N. Y. Yao, and A. Auerbach, *Phys. Rev. B* **93**, 224205 (2016).
- [58] D. J. Luitz and Y. B. Lev, *Phys. Rev. B* **96**, 020406 (2017).
- [59] A. Nahum, J. Ruhman, and D. A. Huse, *Phys. Rev. B* **98**, 035118 (2018).
- [60] S. Xu and B. Swingle, [arXiv:1802.00801](https://arxiv.org/abs/1802.00801).
- [61] C. J. Lin and O. I. Motrunich, *Phys. Rev. B* **97**, 144304 (2018).
- [62] V. Khemani, D. A. Huse, and A. Nahum, *Phys. Rev. B* **98**, 144304 (2018).
- [63] J. J. Mendoza-Arenas, M. Znidaric, V. K. Varma, J. Goold, S. R. Clark, and A. Scardicchio, *Phys. Rev. B* **99**, 094435 (2019).
- [64] G. Vidal, *Phys. Rev. Lett.* **93**, 040502 (2004).
- [65] G. Vidal, *Phys. Rev. Lett.* **91**, 147902 (2003).
- [66] A. J. Daley, C. Kollath, U. Schollwöck, and G. Vidal, *J. Stat. Mech.* (2004) P04005.
- [67] S. R. White and A. E. Feiguin, *Phys. Rev. Lett.* **93**, 076401 (2004).
- [68] See the Supplemental Material at <http://link.aps.org/supplemental/10.1103/PhysRevLett.123.165902> for numerical details, fitting procedures, and the calculations for the phenomenological rare region model.
- [69] S. Xu and B. Swingle, *Phys. Rev. X* **9**, 031048 (2019).
- [70] A. Nahum, S. Vijay, and J. Haah, *Phys. Rev. X* **8**, 021014 (2018).
- [71] C. W. von Keyserlingk, T. Rakovszky, F. Pollmann, and S. L. Sondhi, *Phys. Rev. X* **8**, 021013 (2018).